Large Structural Modulations in Incommensurate Te-III and Se-IV

C. Hejny and M. I. McMahon

School of Physics and Centre for Science at Extreme Conditions, The University of Edinburgh, Mayfield Road, Edinburgh EH9 3JZ, United Kingdom

(Received 20 March 2003; published 20 November 2003)

The high-pressure phase of tellurium, Te-III, is found to have an incommensurate monoclinic structure, superspace group $I'2/m(0q0)s0$, of a type previously unknown in the elements. Te-III is stable from 4.5(2) to 29.2(7) GPa; the previously reported transition to a distinct Te-IV phase at 10.6 GPa is not observed. The incommensurate wave vector of Te-III is strongly pressure dependent and varies in a strongly nonlinear way. Se-IV is found to be isostructural with Te-III.

DOI: 10.1103/PhysRevLett.91.215502 PACS numbers: 61.50.Ks, 62.50.+p

The high-pressure behavior of the group VI element tellurium has long been the subject of considerable interest. Its pressure-induced semiconductor to metal transition [1], its numerous high-pressure phases with low-symmetry structures [2], its dramatic changes in superconductivity temperature [3], its unusual melting curve [4], and the reported structural transition in the high-pressure high-temperature liquid state [4] have prompted many resistivity [1], diffraction [2,5–8], density [9,10], extended x-ray-absorption fine structure spectroscopy [11], optical [12], superconductivity [3,13,14], and theoretical [15,16] studies.

Despite this, the structural behavior of high-pressure Te has remained contentious. The generally accepted transition sequence is Te-I to monoclinic Te-II at ~4 GPa, Te-II to orthorhombic Te-III at ~7 GPa, Te-III to rhombohedral Te-IV at 10.6 GPa, and Te-IV to body-centered cubic (bcc) Te-V at 27G Pa [2]. Te-II is reported to have space group $P2_1$ with a monoclinic angle (β) of ~92° that becomes 90° in orthorhombic Te-III [6], and Te-IV is reported to have the β-Po structure [5]. But this consensus has been disturbed by a recent diffraction study of Te-III and Te-IV to 33 GPa [17], which suggested (i) that Te-III is stable over the whole range from 7 to 27 GPa, and (ii) that Te-III has a different (monoclinic) structure to that previously accepted. In addition, numerous weak reflections were found that are incompatible with either the newly proposed structure for Te-III or the β-Po structure of Te-IV [17].

In view of the importance of determining the true high-pressure structural behavior of Te to aid the interpretation of its high-pressure superconductivity [13] and the high-pressure transition in liquid-Te [8], we have reexamined the structures to 35 GPa using powder and single-crystal x-ray diffraction. We find that Te-III has an incommensurate body-centered monoclinic structure of a type previously unknown in the elements.

Experiments were done on high-purity (99.9999%) Te samples obtained from the Aldrich Chemical Company. The finely ground samples were loaded into diamond anvil cells using 4:1 methanol:ethanol as a pressure transmitting medium [18] and a small ruby sphere for pressure measurement [19]. Powder-diffraction data were collected on station 9.1 at the Synchrotron Radiation Source (SRS), Daresbury Laboratory, using an image-plate area detector and wavelength of 0.4654 Å [20]. The 2D diffraction profiles were integrated azimuthally, and structural data were obtained by Rietveld refinement.

The transition from Te-I to Te-II was observed at 4.0(1) GPa, but the high resolution of the data revealed the transition to Te-III at 4.5(2) GPa, well below the previously reported ~7 GPa. Te-II and Te-III coexist over a wide pressure range on pressure increase, and single-phase patterns of Te-III are observed only above 8.0(5) GPa. A diffraction profile from Te-III at 8.5 GPa is shown in Fig. 1, and is clearly the same as that observed in the recent diffraction study of Te-III by Takumi *et al.* [17]. Observation of diffraction profiles as a function of pressure revealed two different kinds of diffraction peaks—those that remained intense and coalesced at higher pressures and those that remained singlets and decreased in intensity. *Ab initio* indexing of the former showed that they could all be indexed on a body-centered monoclinic (bcm) cell with two atoms per unit cell and

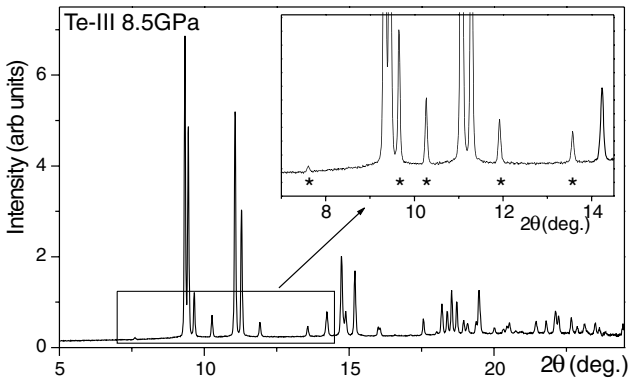

FIG. 1. Diffraction profile from Te-III at 8.5 GPa. The inset shows some of the low-angle reflections (marked with asterisks) whose intensity decreases with increasing pressure, as described in the text.

lattice parameters $a = 3.9189(3)$ Å, $b = 4.7334(4)$ Å, $c = 3.0617(2)$ Å, and $\beta = 113.525(6)°$ at 8.5 GPa. This cell is closely related to those reported previously for Te-III [5,6,17,21].

While the bcm structure explains all the strong diffraction peaks of Te-III, attempts to index the remaining weaker peaks, either as a superlattice or as a separate phase, were unsuccessful. It appeared that single-crystal techniques were needed, but previous attempts had been unable to obtain single-crystal data beyond the first-order transition to Te-II [22]. However, our recent studies of alkali metals have shown that modern detectors and synchrotron radiation enable substantial structural information to be obtained from even quite poor quasisingle crystals of high-pressure phases [23]. Attempts to obtain even a quasisingle crystal of Te-III proved very difficult, but one sample suitable for data collection was eventually obtained out of 29 loadings. Data from this sample at 7.4 GPa were collected on both our in-house charge-coupled device (CCD) diffractometer and on the CCD diffractometer on station 9.8 at SRS, Daresbury, using wavelengths of 0.71 and 0.4815 Å, respectively.

A diffraction pattern from the single crystal of Te-III, which was found to comprise diffraction peaks from two twin components, is shown in Fig. 2. It is immediately apparent that in addition to the strong Bragg reflections from the bcm structure, there are intense satellite reflections at $(h, k \pm q, l)$ with $q \sim 0.3$. The structure of Te-III is thus incommensurate, and all of the reflections in Fig. 1 can be indexed using four integers (h, k, l, m), according to $\vec{H} = h\vec{a}^* + k\vec{b}^* + l\vec{c}^* + mq\vec{b}^*$, where $\{\vec{a}^*, \vec{b}^*, \vec{c}^*\}$ define the reciprocal lattice of the bcm structure, and the incommensurate wave vector is $(0, q = 0.287, 0)$ at 8.5 GPa. Only first-order satellite reflections [mod$(m) = 1$] are observed in Te-III.

We have refined the structure within the formalism of 4D superspace [24] using JANA2000 [25]. Analysis of the systematic absences showed the superspace group to be $I^l2/m(0q0)s0$, where I^l denotes the centering $(\frac{1}{2}, \frac{1}{2}, \frac{1}{2}, \frac{1}{2})$ in superspace [26]. The modulation of the single atom in the structure can be described as $\mathbf{u} = \mathbf{u}(\bar{x}_4)$ where $\bar{x}_4 = \mathbf{q} \cdot \mathbf{r}_0$ is the fourth superspace coordinate, $\mathbf{r}_0 = \mathbf{n} + \mathbf{x}_0$ is the position of the atom in the nth unit cell in the average structure, and $\mathbf{u}$ is its displacement in the real structure. The modulation can then be modeled as a sum of Fourier amplitudes defined by

$$u_\alpha(\bar{x}_4) = \sum_{n=1}^{\infty} [A_{n\alpha} \cos(2\pi n \bar{x}_4) + B_{n\alpha} \sin(2\pi n \bar{x}_4)] \quad (1)$$

$(\alpha = x, y, z)$ and where $A_{n\alpha}$ and $B_{n\alpha}$ are the amplitudes of the nth order Fourier components.

For the refinement of only first-order Fourier components $(n = 1)$, the superspace symmetry of Te-III reduces the number of refinable modulation parameters to two, namely, B_{1x} and B_{1z} [25]. The resulting excellent fit ($R_p = 4.8\%$, $R_{wp} = 6.6\%$, $\chi^2 = 1.53$) to the diffraction profile of Fig. 1 is shown in Fig. 3, and the final refined parameters are $a = 3.9181(1)$ Å, $b = 4.7333(1)$ Å, $c = 3.0612(1)$ Å, $\beta = 113.542(2)°$, $q = 0.2880(2)$, $B_{1x} = 0.0215(9)$, and $B_{1z} = 0.0925(7)$.

Detailed diffraction studies of Te up to 36 GPa showed that Te-III is stable to 29.2(7) GPa, where it transforms directly to bcc Te-V. The satellite peaks, although extremely weak, remain visible up to this transition pressure. No effects of nonhydrostaticity were observed—both satellite and main peaks remained sharp over the entire stability range of Te-III, and the measured peak positions showed no evidence of any deviatoric stress. At 24 GPa, all peak positions fit to better that 0.002 Å. The previously reported phase transition to Te-IV at ~10 GPa [2,5,6] is not observed. We believe that the

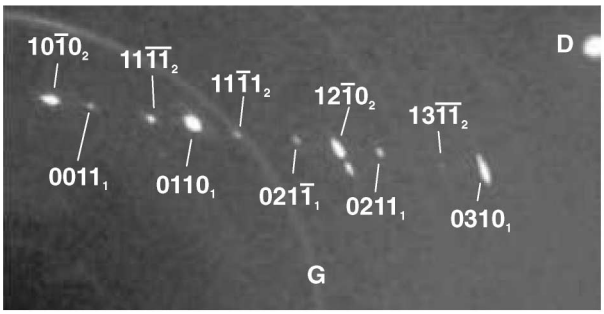

FIG. 2. A diffraction image from a twinned single crystal of Te-III at 7.4 GPa. The main bcm reflections from the two twin components are shown, indexed $(hkl0)_1$ and $(hkl0)_2$, as well as the indexed satellite reflections. A powder line from the tungsten gasket is marked "G," while a reflection from one of the diamond anvils is marked "D."

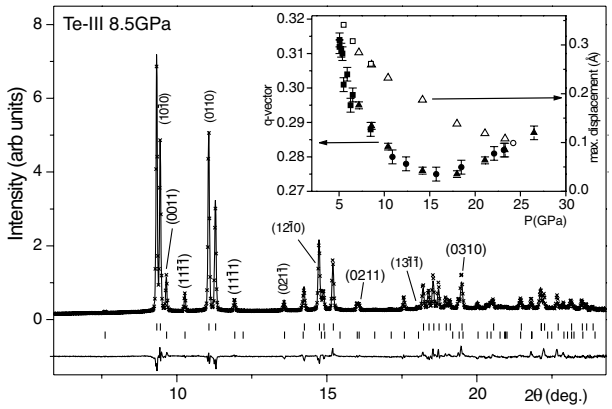

FIG. 3. Rietveld refinement of incommensurate Te-III at 8.5 GPa. The upper and lower tick marks below the profile show the peak positions of the main and first-order satellite reflections, respectively. The reflections shown in Fig. 2 are identified by their indices. The inset shows (i) the pressure dependence of the incommensurate wave vector $(0q0)$, and (ii) the maximum atomic displacement, over the range 5 to ~25 GPa. Data from three different samples are distinguished by different symbols.

poorer resolution of the previous diffraction studies was unable to distinguish diffraction patterns of Te-III from that of the proposed β-Po structure above this pressure. The revised phase transition sequence in Te on compression is therefore Te-I $\rightarrow$ Te-II at 4.0(1) GPa, Te-II $\rightarrow$ Te-III at 4.5(2) GPa, and Te-III $\rightarrow$ Te-V at 29.2(7) GPa.

The inset of Fig. 3 shows the pressure dependence of the incommensurate wave vector, q, of Te-III as a function of pressure. The maximum value of $q = 0.314(2)$ is found at 5 GPa, immediately above Te-II, after which q decreases strongly, reaching a minimum value of 0.274(2) at 15.5(2) GPa. At pressures above this, q increases again, reaching a value of 0.287(2) at 26.5 GPa, the highest pressure at which it could be measured.

Te-III is a new elemental structure type that adds another twist to the remarkable structural complexity discovered in elemental metals in recent work [23]. The maximum atomic displacement of 0.341(2) Å at 5.5 GPa (see inset of Fig. 3) is more than an order of magnitude greater than the displacement of 0.026 Å reported in the low-temperature charge-density wave (CDW) state of uranium [27]—the only element known to have any form of modulated structure at ambient pressure. And while the CDW state is known to vanish at pressures above 1.2 GPa [28], Te-III is stable over a pressure range of $\sim$24 GPa during which its density changes by 18%. The compressibility of Te to 36 GPa is shown in Fig. 4.

The unmodulated bcm structure of Te-III is three dimensionally bonded and each atom is 6-fold coordinated, with two nearest neighbors at 3.100 Å and four at 3.104 Å at 5.5 GPa. The effect of the modulation on these contact distances is shown in Fig. 5(i), where the interatomic distances are plotted as a function of the phase factor t, where t is defined by $\bar{x}_4 = \mathbf{q} \cdot \mathbf{r}_0 + t$, and $\bar{x}_4$ is the argument of the modulation function [24]. While the distance to the two nearest-neighbor (n-n) atoms at 3.100 Å depends only on the c-axis lattice parameter and is therefore unaffected by the modulation, the four atoms at 3.104 Å assume different distances in the modulated structure in the (large) range 2.900(2) to 3.405(2) Å [Fig. 5(i)], with an average bond length of 3.127(2) Å. The modulated structure, shown in the inset of Fig. 4, is still 6-fold coordinated. In the unmodulated bcm structure, all contact distances in the structure would decrease with increasing pressure.

However, refinements of the modulated structure over the range 5.5–23.3 GPa show that the change in the modulation with increasing pressure is such as to make the closest approach distance in the modulated structure, e.g., 2.900 Å at 5.5 GPa, independent of pressure. This is illustrated in Fig. 5(ii) which shows, on the same scale used in Fig. 5(i), the effect of the modulation on the n-n distances at 23.3 GPa. The structure is still 6-fold coordinated, and, while the unmodulated distances have compressed considerably to 2.962 and 2.965 Å, the smaller structural modulation is such that the closest approach distance at 23.3 GPa is 2.897(4) Å, the same, within error, as that at 5.5 GPa. And at all pressures between 5.5 and 23 GPa, the closest-contact distance lies between 2.890(3) and 2.905(3). Therefore, the effect of the structural modulations in Te-III is to create a structure that has a wide range of contact distances, a number of which are considerably shorter ($\sim$0.2 Å) than would be found in the unmodulated bcm structure of the same density, and the shortest of which is in the range 2.890 to 2.905 Å over the entire stability range of Te-III.

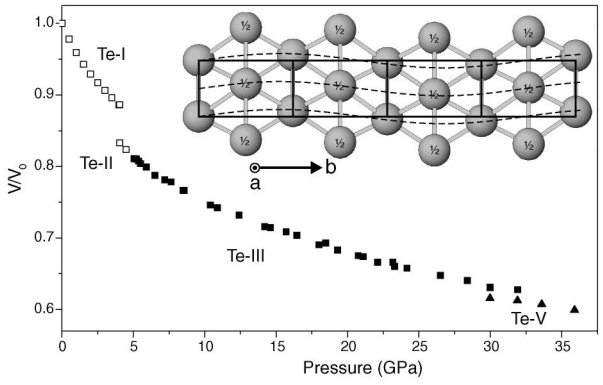

FIG. 4. The compressibility of Te to 36 GPa. The data points below 5 GPa are those from Ref. [10]. The inset shows a view down the a axis of four unit cells of Te-III at 8.5 GPa. The six nearest-neighbor contact distances for each atom are shown, and those atoms at the body centers are labeled with "$\frac{1}{2}$." The modulation wave is indicated by the dotted lines.

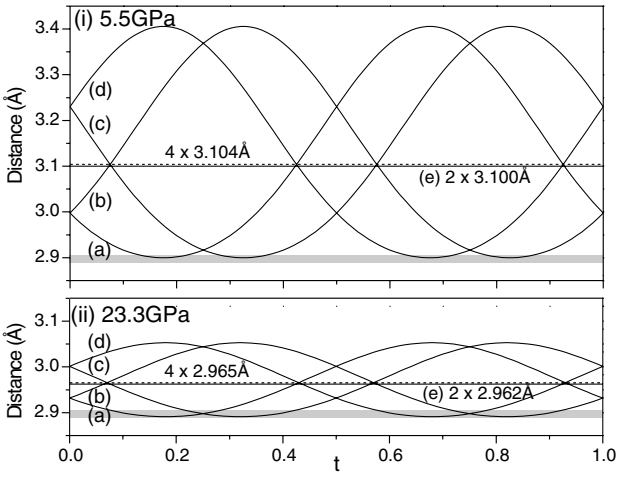

FIG. 5. Nearest-neighbor contact distances in Te-III at (i) 5.5 GPa and (ii) 23.3 GPa as a function of the phase factor, t. The contact distances are from the atom at (000) to the atoms at (a) $(\frac{1}{2}\frac{1}{2}\frac{1}{2})$, ($b$) $(-\frac{1}{2}-\frac{1}{2}-\frac{1}{2})$, ($c$) $(\frac{1}{2}-\frac{1}{2}\frac{1}{2})$, ($d$) $(-\frac{1}{2}\frac{1}{2}-\frac{1}{2})$, and ($e$) (001) and (00 $-$ 1). In the unmodulated structure, the four contact distances (a)–(d) are the same, as marked by the dashed horizontal lines at 3.104 and 2.965 Å in (i) and (ii), respectively. The grey horizontal band between 2.890 to 2.905 Å shows the limits within which the closest-contact distances lie at all pressures between 5.5 and 23.3 GPa.

The present results have interesting implications for interpreting the pressure dependence of the superconducting transition temperature in Te [3,13]: the discontinuity in T_c at ~35 GPa [3] almost certainly arises from the Te-III to Te-V transition, while the smooth decrease of T_c between 8 and 26 GPa [3,13] takes place entirely within the Te-III phase. Intriguingly, our structure refinements show that the rapid decrease in T_c in the pressure range 8–15 GPa [13] is accompanied by the rapid decrease in q to its minimum (see the inset of Fig. 3). Anomalies seen previously in the calculated phonon frequencies in high-pressure Te [16], and not interpretable in terms of the β-Po and bcc structures, also now invite reinterpretation in light of the new structural data.

The phase diagram of tellurium shows Te-III existing up to the melting curve [4]. The incommensurate nature of the structure will then have important implications for studies of liquid-Te (l-Te), where the structures of the crystalline phases are essential in interpreting diffraction data from the liquid phases. At 0 GPa, l-Te has a structure comprising "entangled, broken chains" [29] and a coordination of ~2.5 at the melting temperature. At high pressure, the coordination of l-Te is reported to be predominantly 3-fold between 0 and 5 GPa, increasing to ~4 at 6 GPa [8]. However, this interpretation assumed that crystalline Te-II and Te-III were 4-fold coordinated [6,8]. The 6-fold coordination of Te-III reported in this study, the pressure independence of the closest-contact distance, and the different atomic environment of each atom in the incommensurate structure will open the way to a reinterpretation of the structures of l-Te at high pressure, in particular, those involved in the liquid-liquid phase transition reported at ~4.5 GPa [4].

Finally, previous studies have noted the similarities between the high-pressure behavior of Te and Se [30]. The observation that Te-III is incommensurate raises the obvious question as to whether the same, or a related, structure exists in Se. We note that the Se-IV data of Akahama *et al.* [30] at 34.9 GPa, including the peak from the "extra phase," can be indexed on the Te-III structure with $a = 3.288$ Å, $b = 4.010$ Å, $c = 2.589$ Å, $\beta = 112.98°$, and $q = 0.288$. Our own powder data from Se-IV at 35.0 GPa give $a = 3.2991(2)$ Å, $b = 3.9959(6)$ Å, $c = 2.5869(11)$ Å, $\beta = 113.105(5)°$, $q = 0.288(1)$, $B_{1x} = 0.0249(9)$, and $B_{1z} = 0.1026(8)$.

We acknowledge helpful discussions with Professor R. J. Nelmes and Dr. V. Petricek. We thank Dr. M. Roberts and Dr. S. Teat of Daresbury Laboratory for assistance in setting up the 9.1 and 9.8 beam lines, respectively, and Dr. S. Rekhi for assistance in the early part of this study. This work was supported by grants from EPSRC, funding from CCLRC, and facilities provided by Daresbury Laboratory. M. I. M. acknowledges support from the Royal Society.

[1] P.W. Bridgman, Proc. Am. Acad. Arts Sci. **81**, 167 (1952).
[2] G. Parthasarathy and W. B. Holzapfel, Phys. Rev. B **37**, 8499 (1988).
[3] Y. Akahama, M. Kobayashi, and H. Kawamura, Solid State Commun. **84**, 803 (1992).
[4] V.V. Brazhkin, R. N. Voloshin, S.V. Popova, and A. G. Umnov, J. Phys. Condens. Matter **4**, 1419 (1992).
[5] J. C. Jamieson and D. B. McWhan, J. Chem. Phys. **43**, 1149 (1965).
[6] K. Aoki, O. Shimomura, and S. Minomura, J. Phys. Soc. Jpn. **48**, 551 (1980).
[7] K. Yaoita *et al.*, J. Non-Cryst. Solids **156–158**, 157 (1993).
[8] N. Funamori and K. Tsuji, Phys. Rev. B **65**, 014105 (2001).
[9] Y. Katayama *et al.*, J. Non-Cryst. Solids **156–158**, 687 (1993).
[10] S. N. Vaidya and G. C. Kennedy, J. Phys. Chem. Solids **33**, 1377 (1972).
[11] Y. Katayama, O. Shimomura, and K. Tsuji, J. Non-Cryst. Solids **250–252**, 537 (1999).
[12] H. C. Hsueh *et al.*, Phys. Rev. B **61**, 3851 (2000).
[13] I.V. Berman *et al.*, Sov. Phys. Solid State **14**, 2192 (1973).
[14] F. P. Bundy and K. J. Dunn, Phys. Rev. Lett. **44**, 1623 (1980).
[15] R. Stadler and M. J. Gillan, J. Phys. Condens. Matter **12**, 6053 (2000).
[16] F. Mauri *et al.*, Phys. Rev. Lett. **77**, 1151 (1996).
[17] M. Takumi, T. Masamitsu, and K. Nagata, J. Phys. Condens. Matter **14**, 10 609 (2002).
[18] No reactivity was observed between the tellurium and the pressure medium. Diffraction profiles collected from the known phases Te-I and Te-V, including samples downloaded to Te-I after lengthy experiments, contained no additional peaks from contaminant phases.
[19] H. K. Mao *et al.*, J. Geophys. Res. **91**, 4673 (1986).
[20] R. J. Nelmes and M. I. McMahon, J. Synchrotron Radiat. **1**, 69 (1994).
[21] The relationship between the cells of Jamieson and McWhan (J), Aoki *et al.* (A), and (T), with the present bcm cell (I), are $\vec{a}_J = \vec{a}_I + \vec{c}_I$, $\vec{b}_J = -\vec{b}_I$, and $\vec{c}_J = -\vec{c}_I$; $\vec{a}_A = \vec{c}_I$, $\vec{b}_A = 2\vec{a}_I + \vec{c}_I$, and $\vec{c}_A = \vec{b}_I$; and $\vec{a}_T = \vec{a}_I + 3\vec{c}_I$, $\vec{b}_T = -\vec{b}_I$, and $\vec{c}_T = \vec{a}_I$, respectively.
[22] R. Keller *et al.*, Phys. Rev. B **16**, 4404 (1977).
[23] R. J. Nelmes *et al.*, Phys. Rev. Lett. **88**, 155503 (2002).
[24] S. van Smaalen, Crystallogr. Review **4**, 79 (1995).
[25] V. Petricek and M. Dusek, *The Crystallographic Computing System JANA2000* (Institute of Physics, Praha, Czech Republic, 2000).
[26] We have chosen this nonstandard space-group setting rather than the standard $C2/m(0q0)s0$ with $q \sim 0.7$ setting so as to simplify the description of the transition from Te-III to Te-II, to be published in a later paper.
[27] S. van Smaalen and T. F. George, Phys. Rev. B **35**, 7939 (1987).
[28] T. F. Smith and E. S. Fisher, J. Low Temp. Phys. **12**, 631 (1973).
[29] J. Hafner, J. Phys. Condens. Matter **2**, 1271 (1990), and references therein.
[30] Y. Akahama, M. Kobayashi, and H. Kawamura, Solid State Commun. **83**, 269 (1992).